

## Electronic Supplementary Information (ESI)

**Mixed (porphyrinato)(phthalocyaninato) rare-earth(III) double-decker complexes for broadband light harvesting organic solar cells**

*Yong Li, Yongzhong Bian,\* Ming Yan, Prem S. Thapaliya, Daniel Johns, Xingzhong Yan,\* David Galipeau, and Jianzhuang Jiang\**

## S1. Experimental Section

*General:* *n*-Octanol was distilled from sodium under nitrogen. Dichloromethane ( $\text{CH}_2\text{Cl}_2$ ) for spectroscopic studies was freshly distilled from  $\text{CaH}_2$  under  $\text{N}_2$ . All other reagents and solvents were used as received from vendors. Column chromatography was carried out on silica gel (Merck, Kieselgel 60, 70–230 mesh) columns with the indicated eluents to isolate and purify the title complexes. The compounds  $[\text{M}(\text{acac})_3] \cdot n\text{H}_2\text{O}$ ,  $\text{H}_2\text{TCIPP}$ , and  $\text{H}_2\text{Pc}(\alpha\text{-OC}_4\text{H}_9)_8$  were prepared according to the published procedures.<sup>[S1–S3]</sup>

$^1\text{H}$  NMR spectra were recorded on a Bruker Avance 400 NMR spectrometer in  $\text{CDCl}_3/\text{DMSO-d}_6$  (1/1, v/v) in the presence of *ca.* 1% (by volume) hydrazine hydrate. Spectra were referenced internally to the residual solvent resonance at chemical shift ( $\delta$ ) of 2.50 (DMSO- $d_6$ , 5 peaks with  $J = 1.9$  Hz). MALDI-TOF mass spectra were taken on a Bruker BIFLEX III ultrahigh-resolution Fourier transform ion cyclotron resonance (FT-ICR) mass spectrometer with  $\alpha$ -cyano-4-hydroxycinnamic acid as a matrix. Elemental analyses were performed on Flash EA 1112 Elemental Analyzer. IR spectra were recorded in KBr matrix pellets on a BIORAD FTS-165 spectrometer with a spectral resolution of 2  $\text{cm}^{-1}$ .

*General procedures for the preparation of  $[\text{M}^{III}\text{H}(\text{TCIPP})\{\text{Pc}(\alpha\text{-OC}_4\text{H}_9)_8\}]$  ( $\text{M} = \text{Sm, Eu, Tb, Dy, Ho, Lu; 2–7}$ ):* A mixture of  $[\text{M}^{III}(\text{acac})_3] \cdot n\text{H}_2\text{O}$  ( $\text{M} = \text{Sm, Eu, Tb, Dy, Ho, Lu}$ ) (0.06 mmol) and  $\text{H}_2\text{TCIPP}$  (37.6 mg, 0.05 mmol) in *n*-octanol (4 mL) was heated to reflux under a slow stream of nitrogen for *ca.* 6 h. The mixture was cooled to room temperature, and then treated with  $\text{H}_2[\text{Pc}(\alpha\text{-OC}_4\text{H}_9)_8]$  (54.6 mg, 0.05 mmol) under reflux for another 70 minutes. After a brief cooling, the mixture was evaporated under reduced pressure and the residue was subjected to chromatography on a silica gel column. A small amount of unreacted  $\text{H}_2\text{TCIPP}$  was separated by using  $\text{CHCl}_3/\text{hexane}$  (5:1, v/v). The column was eluted with  $\text{CHCl}_3/\text{MeOH}$  (98:2, v/v), and a small green band containing the metal-free phthalocyanine was developed and separated. The column was further eluted with  $\text{CHCl}_3/\text{MeOH}$  (95:5, v/v), another green band containing the protonated double-decker was developed, collected and evaporated. No nonprotonated counterpart was detected during chromatography. The crude product was purified by repeated chromatography followed by recrystallization from  $\text{CHCl}_3/\text{MeOH}$ .

For **2**: yield: 52%.  $^1\text{H}$  NMR (400 MHz,  $\text{CDCl}_3/\text{DMSO-d}_6$  (1/1, v/v) with *ca.* 1% hydrazine hydrate, 294.2 K):  $\delta$  8.22 (s, 8H, Por,  $\text{H}_\beta$ ), 7.68 (s, 8H, Pc,  $\text{H}_\beta$ ), 7.40–7.60 (m, 4H, Por,  $\text{H}_{\text{aryl}}$ ), 7.04–7.06 (m, 8H, Por,  $\text{H}_{\text{aryl}}$ ), 6.82 (m, 4H, Por,  $\text{H}_{\text{aryl}}$ ), 5.95 (m, 4H, Por,

H<sub>aryl</sub>), 4.75-5.40 [m, 16H, Pc( $\alpha$ -OC<sub>4</sub>H<sub>9</sub>)<sub>8</sub>, -OCH<sub>2</sub>-], 1.40-1.80 [m, 32H, Pc( $\alpha$ -OC<sub>4</sub>H<sub>9</sub>)<sub>8</sub>, -CH<sub>2</sub>-], 0.90 [m, 24H, Pc( $\alpha$ -OC<sub>4</sub>H<sub>9</sub>)<sub>8</sub>, -CH<sub>3</sub>]. UV/Vis (CHCl<sub>3</sub>):  $\lambda_{\text{max}}/\text{nm}$  (log  $\varepsilon$ ) = 323 (4.92), 422 (5.52), 498 (4.75), 571 (4.30), 622 (4.58), 852 (shoulder, sh), 925 (4.48). MS (MALDI-TOF): an isotopic cluster peaking at *m/z* 1992.4 [Calcd. for (MH)<sup>+</sup> 1992.6]. Anal. Calcd. (%) for C<sub>108</sub>H<sub>105</sub>O<sub>8</sub>N<sub>12</sub>Cl<sub>4</sub>Sm·0.25CHCl<sub>3</sub>: C, 64.33; H, 5.25; N, 8.32. Found: C, 64.25; H, 5.38; N, 8.33.

For **3**: yield: 63%. <sup>1</sup>H NMR (400 MHz, CDCl<sub>3</sub>/DMSO-d<sub>6</sub> (1/1, v/v) with *ca.* 1% hydrazine hydrate, 300.0 K):  $\delta$  8.22 (s, 8H, Por, H<sub>B</sub>), 7.68 (s, 8H, Pc, H<sub>B</sub>), 7.29 (m, 4H, Por, H<sub>aryl</sub>), 6.90 (m, 8H, Por, H<sub>aryl</sub>), 6.60 (m, 4H, Por, H<sub>aryl</sub>), 6.25 (m, 4H, Por, H<sub>aryl</sub>), 4.65-5.40 [m, 16H, Pc( $\alpha$ -OC<sub>4</sub>H<sub>9</sub>)<sub>8</sub>, -OCH<sub>2</sub>-], 1.40-1.80 [m, 32H, Pc( $\alpha$ -OC<sub>4</sub>H<sub>9</sub>)<sub>8</sub>, -CH<sub>2</sub>-], 1.00-1.20 [m, 24H, Pc( $\alpha$ -OC<sub>4</sub>H<sub>9</sub>)<sub>8</sub>, -CH<sub>3</sub>]. UV/Vis (CHCl<sub>3</sub>):  $\lambda_{\text{max}}/\text{nm}$  (log  $\varepsilon$ ) = 324 (4.89), 420 (5.47), 499 (4.74), 571 (4.25), 624 (4.56), 855 (sh), 931 (4.45). MS (MALDI-TOF): an isotopic cluster peaking at *m/z* 1993.2 [Calcd. for (MH)<sup>+</sup> 1993.6]. Anal. Calcd. (%) for C<sub>108</sub>H<sub>105</sub>O<sub>8</sub>N<sub>12</sub>Cl<sub>4</sub>Eu·0.25CHCl<sub>3</sub>: C, 64.28; H, 5.24; N, 8.31. Found: C, 64.43; H, 5.40; N, 8.39.

For **4**: yield: 61%. UV/Vis (CHCl<sub>3</sub>):  $\lambda_{\text{max}}/\text{nm}$  (log  $\varepsilon$ ) = 323 (4.79), 418 (5.35), 496 (4.66), 571 (4.17), 625 (4.47), 866 (sh), 946 (4.30). MS (MALDI-TOF): an isotopic cluster peaking at *m/z* 2000.1 [Calcd. for (MH)<sup>+</sup> 2000.6]. Anal. Calcd. (%) for C<sub>108</sub>H<sub>105</sub>O<sub>8</sub>N<sub>12</sub>Cl<sub>4</sub>Tb·0.25CHCl<sub>3</sub>: C, 64.06; H, 5.23; N, 8.28. Found: C, 64.13; H, 5.27; N, 8.21.

For **5**: yield: 57%. UV/Vis (CHCl<sub>3</sub>):  $\lambda_{\text{max}}/\text{nm}$  (log  $\varepsilon$ ) = 323 (4.89), 418 (5.45), 496 (4.78), 571 (4.26), 626 (4.59), 876 (sh), 952 (4.34). MS (MALDI-TOF): an isotopic cluster peaking at *m/z* 2004.8 [Calcd. for (MH)<sup>+</sup> 2004.6]. Anal. Calcd. (%) for C<sub>108</sub>H<sub>105</sub>O<sub>8</sub>N<sub>12</sub>Cl<sub>4</sub>Dy: C, 64.75; H, 5.28; N, 8.39. Found: C, 65.32; H, 5.46; N, 8.41.

For **6**: yield: 45%. UV/Vis (CHCl<sub>3</sub>):  $\lambda_{\text{max}}/\text{nm}$  (log  $\varepsilon$ ) = 323 (4.91), 418 (5.47), 495 (4.84), 571 (4.32), 626 (4.62), 882 (sh), 958 (4.37). MS (MALDI-TOF): an isotopic cluster peaking at *m/z* 2006.3 [Calcd. for (MH)<sup>+</sup> 2006.6]. Anal. Calcd. (%) for C<sub>108</sub>H<sub>105</sub>O<sub>8</sub>N<sub>12</sub>Cl<sub>4</sub>Ho·0.25CHCl<sub>3</sub>: C, 63.87; H, 5.21; N, 8.26. Found: C, 63.67; H, 5.32; N, 8.38.

For **7**: yield: 37%. <sup>1</sup>H NMR (400 MHz, CDCl<sub>3</sub>/DMSO-d<sub>6</sub> (1/1, v/v) with *ca.* 1% hydrazine hydrate, 300.0 K):  $\delta$  7.85 (m, 8H, Por, H<sub>B</sub>), 7.45-7.60 (m, 4H, Por, H<sub>aryl</sub>), 7.43 (s, 8H, Pc, H<sub>B</sub>), 7.08 (s, 4H, Por, H<sub>aryl</sub>), 7.06 (s, 4H, Por, H<sub>aryl</sub>), 6.35 (m, 8H, Por, H<sub>aryl</sub>), 4.60-5.40 [m, 16H, Pc( $\alpha$ -OC<sub>4</sub>H<sub>9</sub>)<sub>8</sub>, -OCH<sub>2</sub>-], 1.40-1.80 [m, 32H, Pc( $\alpha$ -OC<sub>4</sub>H<sub>9</sub>)<sub>8</sub>, -CH<sub>2</sub>-], 1.07 [m, 24H, Pc( $\alpha$ -OC<sub>4</sub>H<sub>9</sub>)<sub>8</sub>, -CH<sub>3</sub>]. UV/Vis (CHCl<sub>3</sub>):  $\lambda_{\text{max}}/\text{nm}$  (log  $\varepsilon$ ) = 324 (5.00), 417 (5.51),

496 (4.95), 571 (4.36), 630 (4.74), 895 (sh), 982 (4.43). MS (MALDI-TOF): an isotopic cluster peaking at  $m/z$  2016.5 [Calcd. for  $(M\text{H})^+$  2016.6]. Anal. Calcd. (%) for  $\text{C}_{108}\text{H}_{105}\text{O}_8\text{N}_{12}\text{Cl}_4\text{Lu}$ : C, 64.35; H, 5.25; N, 8.34. Found: C, 64.04; H, 5.32; N, 8.38.

*Absorption data for complexes 1, 8, 9:*

For **1**: UV/Vis ( $\text{CHCl}_3$ ):  $\lambda_{\text{max}}/\text{nm}$  ( $\log \varepsilon$ ) = 323 (4.85), 418 (5.40), 498 (4.75), 571 (4.20), 627 (4.56), 848 (sh), 954 (4.20).<sup>[S4]</sup>

For **8**: UV/Vis ( $\text{CHCl}_3$ ):  $\lambda_{\text{max}}/\text{nm}$  ( $\log \varepsilon$ ) = 332 (4.92), 401 (5.03), 470 (4.70), 732 (3.55), 1034 (3.79), 1238 (3.91), 1656 (3.49).<sup>[S8]</sup>

For **9**: UV/Vis ( $\text{CHCl}_3$ ):  $\lambda_{\text{max}}/\text{nm}$  ( $\log \varepsilon$ ) = 330 (5.03), 496 (4.24), 557 (4.21), 697 (5.17), 764 (4.37), 859 (sh).

*Femtosecond time-resolved fluorescence measurements:* Time-resolved fluorescence measurements for complexes **1–7** in solution were carried out by using a femtosecond fluorescence upconversion (FFU) technique. The solutions were prepared with anhydrous, deoxygenated  $\text{CH}_2\text{Cl}_2$  at a concentration of ~0.2 mg/mL. The FFU system used in this work is a FOG 100 system (CDP, Russia) with a mode-locked Ti-sapphire laser (Tsunami, Spectra Physics) light source pumped by a 10-W CWNd:YVO<sub>4</sub> laser (Millennia, Spectra-Physics). Briefly, the samples were excited by the second harmonic light (420 nm) generated by doubling a fundamental light at a wavelength of ~840 nm from the mode-locked Ti-sapphire laser with a pulse width of ~57 fs and a pulse repetition rate of 86 MHz, through a  $\beta$ -barium borate nonlinear crystal. The output spectrum of the laser radiation was monitored with a spectrum analyzer (Ocean Optics), to ensure pure mode-locking regime of the femtosecond laser. The polarization of the excitation beam for anisotropy measurements was controlled by a Berek's plate. The sample was rotated to avoid possible photo-degradation and other accumulative effects. The fluorescence emitted from the sample was collected with an achromatic lens and then directed onto another  $\beta$ -barium borate nonlinear crystal. The fundamental light passed through a motorized optical delay line and then mixed with the sample emission in the nonlinear crystal to generate a sum frequency light. The sum frequency light was dispersed by a monochromator and detected via a photomultiplier tube (Hamamatsu R1527P). The instrument response function (IRF) was estimated to be ~250 fs (full-width at half maximum, FWHM). The fluorescence data were fitted with a multi-exponential decay/rise model, in which the fluorescence signal  $F(t)$  can be theoretically expressed by convolution

of the IRF  $r(t)$  with a molecule-response function  $f(\tau)$ ,

$$F(t) = \int_0^\infty r(t-\tau)f(\tau)d\tau \quad (\text{Equation S1})$$

where  $r(t)$  is a Gaussian function with laser pulse width and  $f(\tau)$  is given by:

$$f(\tau) = \sum_i A_i \exp\left(-\frac{\tau}{\tau_i}\right) + A_{\text{offset}} \quad (\text{Equation S2})$$

where the factor  $A$  represents the relative weights (or amplitudes) of the corresponding components, whose sign can distinguish rising or decay process;  $\tau$  is the rising or decay time constant, and  $A_{\text{offset}}$  is a small constant of 2%.

## S2. Results and Discussion

*Synthesis and characterization of 2–7:* The synthesis of mixed (porphyrinato)(phthalocyaninato) rare-earth double-decker complexes  $[\text{M}^{\text{III}}\text{H}(\text{TCIPP})\{\text{Pc}(\alpha\text{-OC}_4\text{H}_9)_8\}]$  ( $\text{M} = \text{Sm}, \text{Eu}, \text{Tb}, \text{Dy}, \text{Ho}, \text{Lu}$ ; **2–7**) involves the prior generation of the half-sandwich complex  $[\text{M}^{\text{III}}(\text{TCIPP})(\text{acac})]$  from  $[\text{M}(\text{acac})_3] \cdot n\text{H}_2\text{O}$  and  $\text{H}_2\text{TCIPP}$ , followed by treatment with metal-free phthalocyanine  $[\text{H}_2\text{Pc}(\alpha\text{-OC}_4\text{H}_9)_8]$  (**Fig. S1**). Consistent with previous reports,<sup>[S4–S5]</sup> only protonated species  $\text{M}^{\text{III}}\text{H}(\text{TCIPP})\{\text{Pc}(\alpha\text{-OC}_4\text{H}_9)_8\}$  (**2–7**) were isolated in good yields since non-peripherally octakis(butyloxy)-substituted phthalocyanine  $[\text{H}_2\text{Pc}(\alpha\text{-OC}_4\text{H}_9)_8]$  got involved in the synthesis of mixed ring rare-earth double-decker complexes. The yields of these compounds show dependence on the size of metal centers. The yield increases from 52% (for  $\text{M} = \text{Sm}$ ) to 63% (for  $\text{M} = \text{Eu}$ ), and then decreases steadily to 37% (for  $\text{M} = \text{Lu}$ ). It was noted that the yield of bis(porphyrinato) rare-earth complexes  $[\text{M}^{\text{III}}(\text{OEP})_2]$  ( $\text{OEP} = \text{octaethylporphyrinate}$ ) decreases gradually along with the contraction of the lanthanides,<sup>[S6]</sup> while an opposite trend was observed for the phthalocyaninato analogues  $[\text{M}^{\text{III}}(\text{Pc})_2]$ .<sup>[S7]</sup> It seems that mid-lanthanides have the appropriate size to optimize the separation of the two macrocyclic ligands in the mixed-ring double-decker complexes  $[\text{M}^{\text{III}}\text{H}(\text{TCIPP})\{\text{Pc}(\alpha\text{-OC}_4\text{H}_9)_8\}]$ , leading to a balance between the stabilization due to  $\pi\text{-}\pi$  interactions and the destabilization due to axial compression of the two  $\pi$  systems. As a result, complexes of mid-lanthanides are relatively more stable and thus can be prepared in higher yield. Similar phenomenon was also observed during the synthesis of neutral mixed (porphyrinato)(phthalocyaninato) rare-earth complexes  $[\text{M}^{\text{III}}(\text{TCIPP})(\text{Pc})]$  in our previous work, of which the yttrium complex exhibited the highest yield though.<sup>[S8]</sup>

All the newly prepared double-decker complexes **2–7** were characterized by elemental analysis and various spectroscopic methods. Satisfactory elemental analysis

results were obtained for all the six protonated mixed (porphyrinato)(phthalocyaninato) rare-earth double-decker complexes. These six compounds were further characterized by MALDI-TOF mass and  $^1\text{H}$  NMR spectroscopic methods. The MALDI-TOF mass spectra of these compounds clearly showed intense signals for the protonated molecular ions ( $[\text{MH}]^+$ ). The isotopic pattern is in good agreement with the simulated one as exemplified by the spectrum of the protonated samarium complex **2** given in **Fig. S2**. Due to the presence of the unpaired electron and/or the paramagnetic nature of some of the rare-earth ions, the  $^1\text{H}$  NMR data for bis(tetrapyrrole) rare-earth(III) complexes are difficult to record. Satisfactory  $^1\text{H}$  NMR spectra couldn't be obtained for the protonated double deckers maybe because of the tautomerization of the acidic proton either on the porphyrin ligand or on the phthalocyanine ligand in these double deckers. In our recent work, it has been revealed that the acid proton in the protonated mixed ring double-decker complexes locates on the porphyrin side other than the phthalocyanine side.<sup>[S9]</sup> Upon addition of *ca.* 1% hydrazine hydrate, well-resolved spectra with all the expected signals were observed for **2**, **3**, and **7**. The IR spectra of **2–7** showed a distinct band at *ca.* 1321–1325  $\text{cm}^{-1}$  (**Fig. S3**), which is a characteristic signal for dianionic phthalocyaninato ligands.<sup>[S4–S5]</sup> The TCIPP $^{\bullet-}$  marker band usually located at 1270–1300  $\text{cm}^{-1}$  was not observed.<sup>[S4]</sup> These results confirmed the dianionic nature of both of the macrocycles and the protonated form of these mixed ring double-decker complexes.

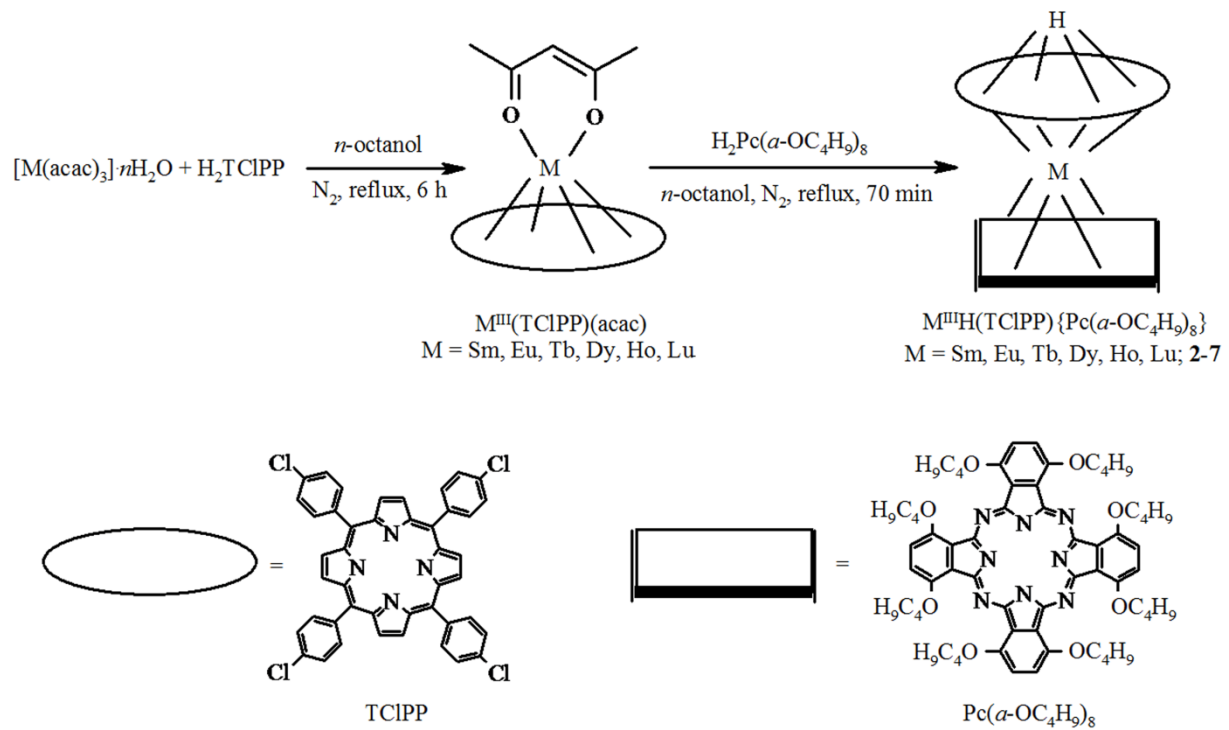


**Fig. S1.** Synthesis of the mixed (porphyrinato)(phthalocyaninato) rare-earth(III) double-decker complexes **2-7**.

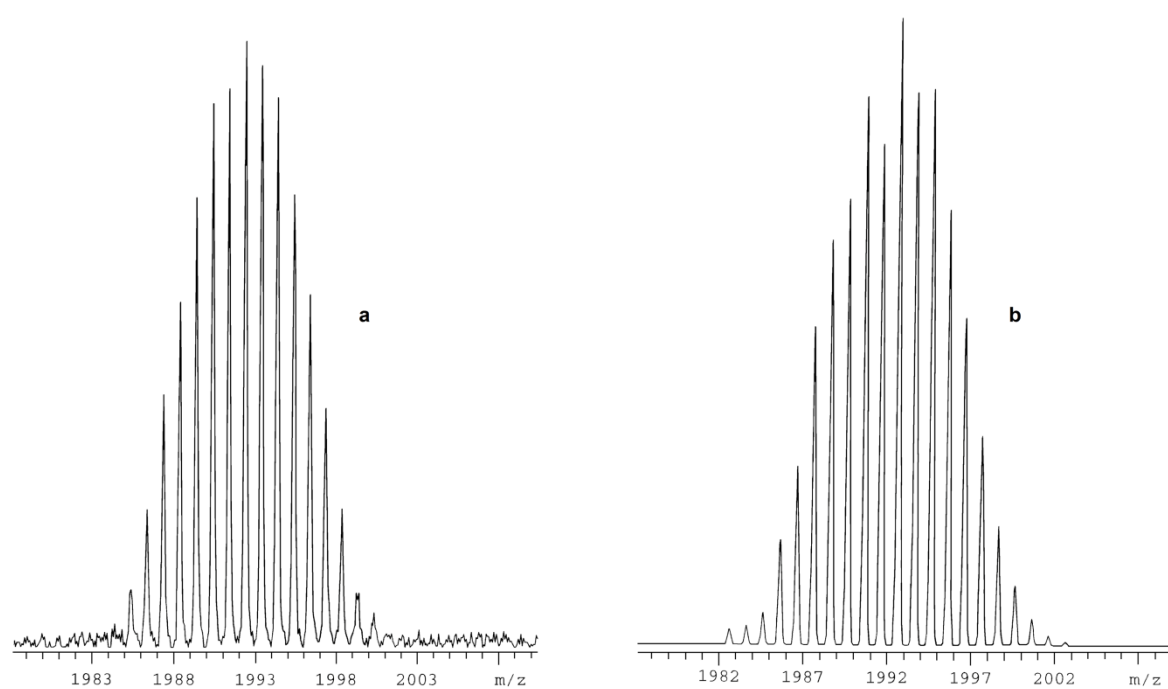


**Fig. S2.** (a) Experimental and (b) simulated isotopic pattern for  $[MH]^+$  of **2** in the MALDI-TOF mass spectrum.

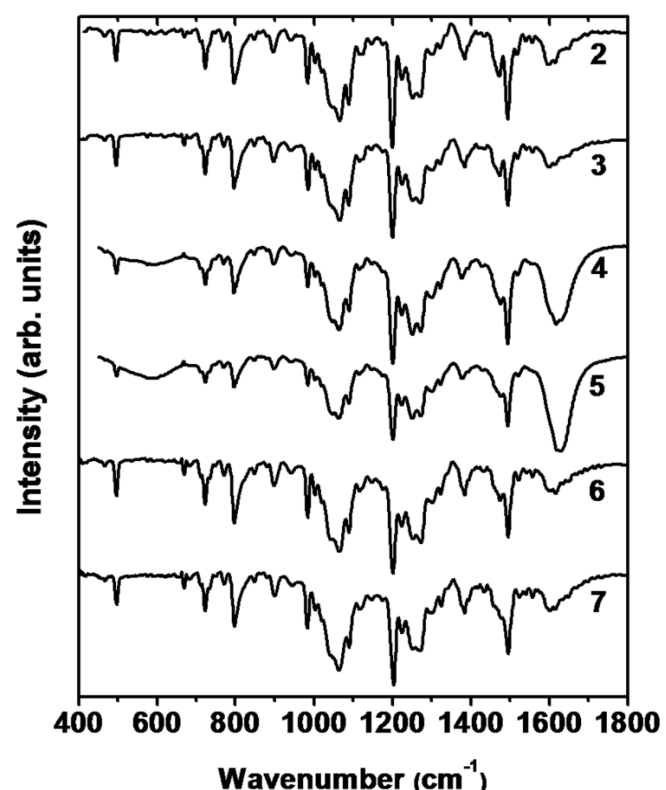


**Fig. S3.** IR spectra of the mixed-ring double-decker complexes 2–7.

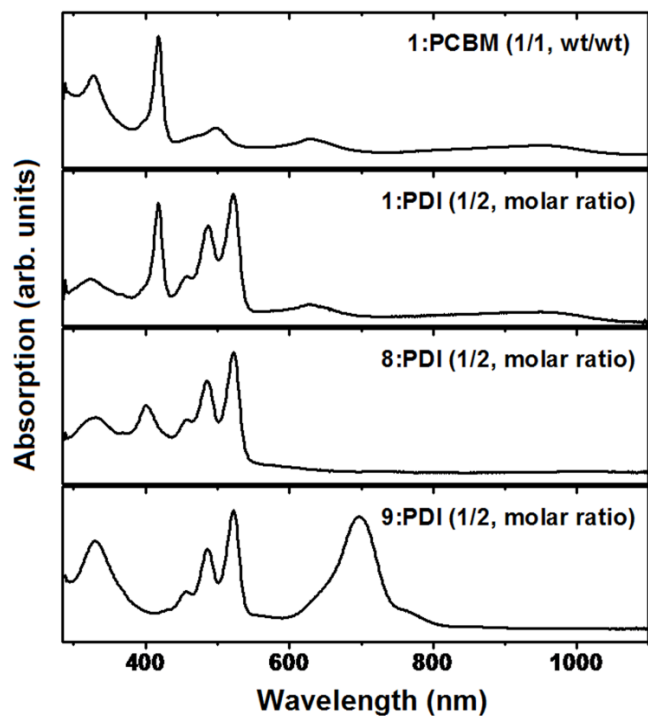


**Fig. S4.** Absorption spectra of mixtures **1**:PCBM (1:1, wt/wt), and double-decker complex (**1**, **8**, and **9**):PDI (1:2, molar ratio) in  $\text{CH}_2\text{Cl}_2$ .

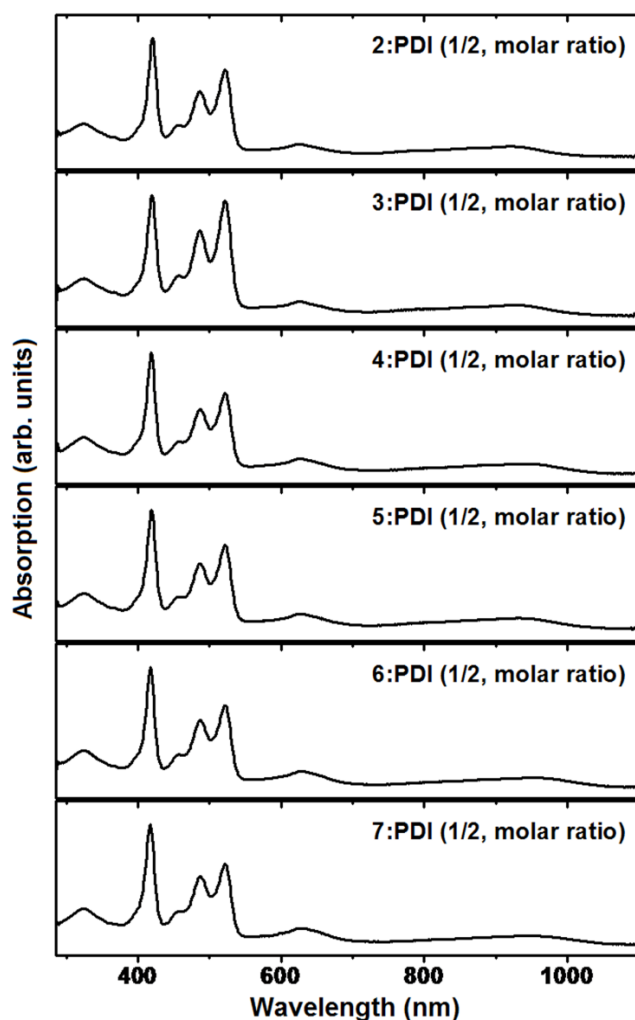


**Fig. S5.** Absorption spectra of mixtures of double-decker complex (2–7):PDI (1:2, molar ratio) in  $\text{CH}_2\text{Cl}_2$ .

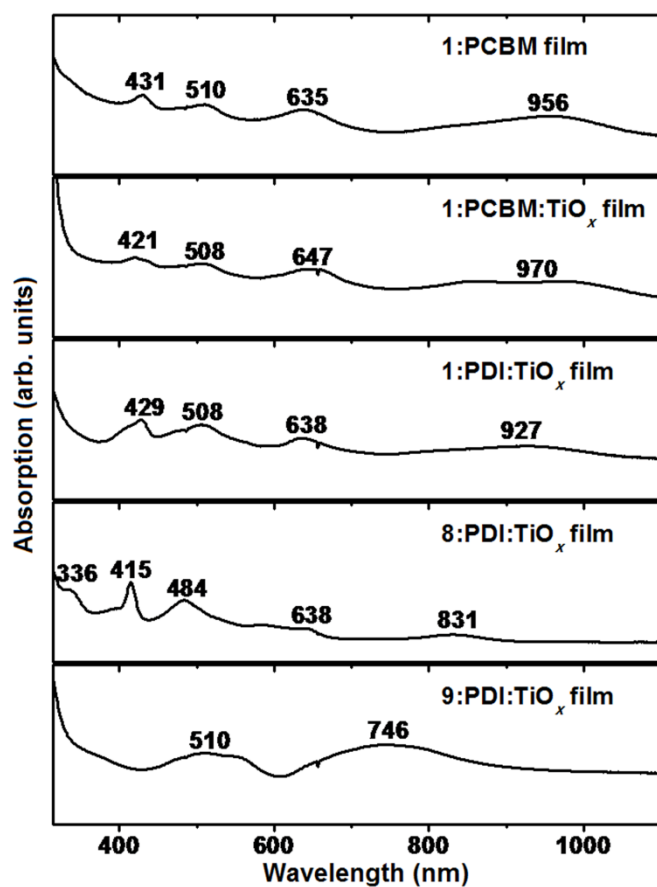


**Fig. S6.** Absorption spectra of the active layers of **1**:PCBM, **1**:PCBM:TiO<sub>x</sub>, **8**:PDI:TiO<sub>x</sub>, and **9**:PDI:TiO<sub>x</sub> on ITO substrates.

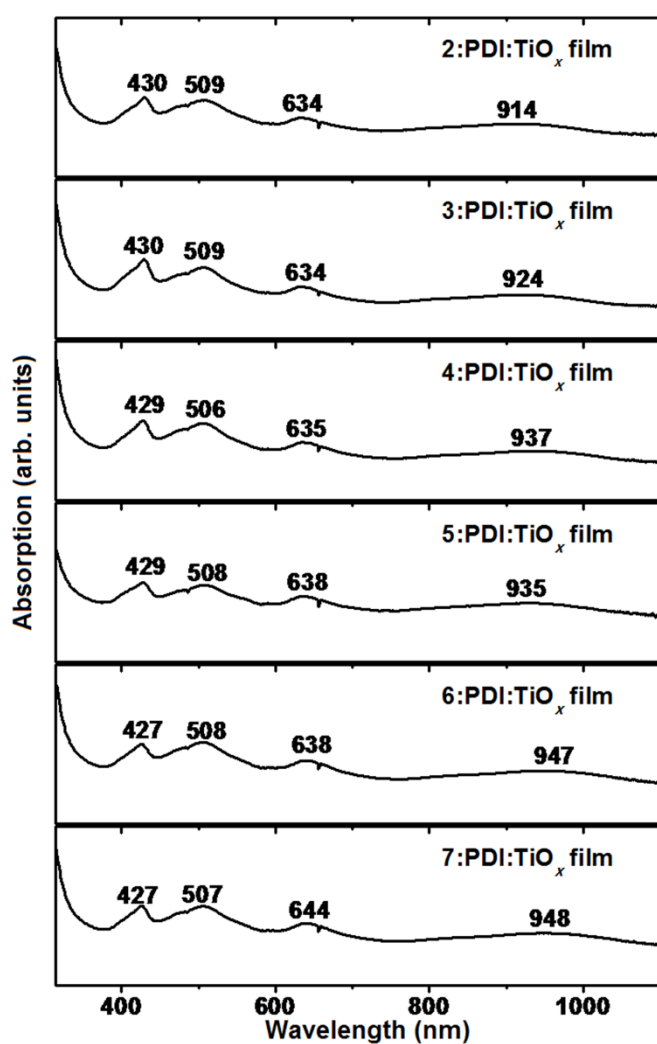


**Fig. S7.** Absorption spectra of the active layers of (2–7):PDI: $\text{TiO}_x$  on ITO glass substrates.

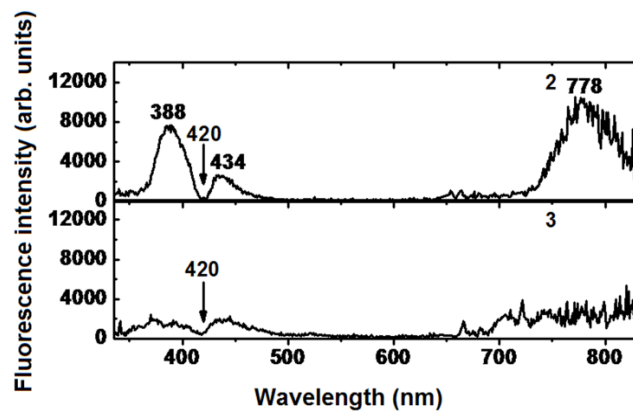


**Fig. S8.** Emission spectra of **2-3** under the 324 nm excitation in  $\text{CH}_2\text{Cl}_2$  solution at room temperature.

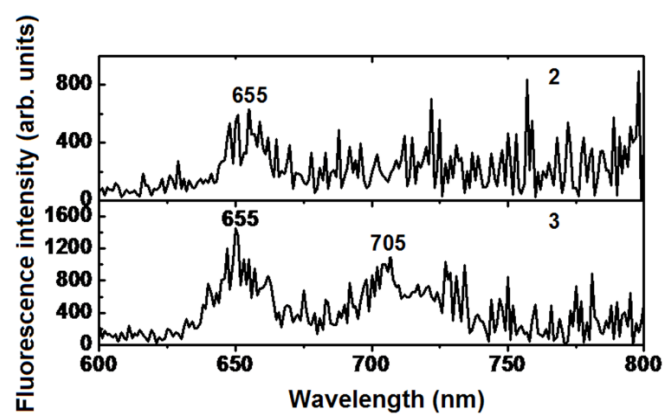


**Fig. S9.** Emission spectra of **2–3** under the 420 nm excitation in  $\text{CH}_2\text{Cl}_2$  solution at room temperature.

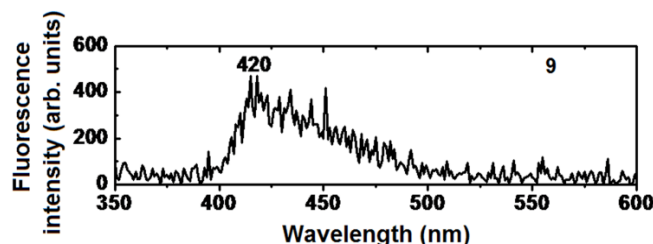


**Fig. S10.** Emission spectrum of **9** under the 330 nm excitation in  $\text{CH}_2\text{Cl}_2$  solution at room temperature.

## References

- [S1] J. G. Stites, C. N. McCarty, L. L. Quill, *J. Am. Chem. Soc.* **1948**, *70*, 3142.
- [S2] G. H. Barnett, M. F. Hudson, K. M. Smith, *J. Chem. Soc., Perkin Trans. I* **1975**, 1401.
- [S3] M. J. Cook, A. J. Dunn, S. D. Howe, A. J. Thomson, K. J. Harrison, *J. Chem. Soc., Perkin Trans. I* **1988**, 2453.
- [S4] R. Wang, R. Li, Y. Li, X. Zhang, P. Zhu, P.-C. Lo, D. K. P. Ng, N. Pan, C. Ma, N. Kobayashi, J. Jiang, *Chem. Eur. J.* **2006**, *12*, 1475.
- [S5] X. Zhang, Y. Li, D. Qi, J. Jiang, X. Yan, Y. Bian, *J. Phys. Chem. B* **2010**, *114*, 13143.
- [S6] J. W. Buchler, J. Hüttermann, J. Löffler, *Bull. Chem. Soc. Jpn.* **1988**, *61*, 71.
- [S7] G. Clarisse, M. T. Riou, *Inorg. Chim. Acta* **1987**, *130*, 139.
- [S8] F. Lu, X. Sun, R. Li, D. Liang, P. Zhu, C.-F. Choi, D. K. P. Ng, T. Fukuda, N. Kobayashi, M. Bai, C. Ma, J. Jiang, *New J. Chem.* **2004**, *28*, 1116.
- [S9] Y. Zhang, X. Cai, P. Yao, H. Xu, Y. Bian, J. Jiang, *Chem. Eur. J.* **2007**, *13*, 9503.